Online Supplementary Material for *A novel body plan alters diversification of body shape and genitalia in live-bearing fish*

R.B. Langerhans and E. Rosa-Molinar

SUPPLEMENTARY TEXT

Sperm Extraction

We confirmed that visually determined genital contact during copulation attempts provides an adequate surrogate for mating success using sperm retrieval from the female reproductive tract. For each preserved female, we followed standard protocols for sperm extraction in female poeciliid fishes (e.g., Evans et al., 2003; Schupp and Plath, 2005). Briefly, under a stereomicroscope we inserted the tip of a Drummond micropipette into the female urogenital opening to flush and retrieve 3 mL of physiological solution (NaCl 0.9%), and repeated this procedure five times. The solution was transferred to an Eppendorf tube, gently shaken to break up the spermatozeugmata, and then examined using a haematocytometer. We scored each female as either having (1) or not having (0) sperm present in the reproductive tract. While this technique may not have fully recovered sperm in all cases, and it is possible that sperm rejection could have occurred, positive cases are unambiguous evidence of successful insemination.

Using this estimate of insemination success as the dependent variable, we conducted a logistic regression to determine whether genital contact significantly predicted insemination success. We performed three separate models, one for each measurement of mating success (genital contact success, number of genital contacts, and genital contact efficiency). We found that all three estimates of mating success significantly predicted sperm presence in the female reproductive tract (genital contact success: $P = 0.0276$, number of genital contacts: $P = 0.0199$, and genital contact efficiency: $P = 0.0030$). Not only did we only find sperm in females where we had observed genital contact, but based on the odds ratios from the models, the odds of insemination increased by 37% for each genital contact observed, and a male with perfect contact efficiency had 197 times higher likelihood of insemination compared to a male showing no appropriate genital contact. Altogether, this provides strong evidence that visually-assessed genital contact during the 30-min mating trials can serve as a meaningful approximation of insemination success after 1 hr of mating.

Phylogenetic Analyses

We used MrBayes 3.1.2 (Ronquist and Huelsenbeck, 2003) to construct phylogenetic hypotheses using the two molecular datasets. We employed six data partitions for the mtDNA analysis (one for each codon of the ND2 and cyt *b* genes) and a single partition for the nDNA analysis. The optimal maximum-likelihood model of sequence evolution was determined for each data partition using jModelTest 0.1.1 (Posada, 2008). We performed partitioned mixed-model Bayesian analyses, where each data partition was assigned its own evolutionary model, with model parameter values being "unlinked" among partitions assigned the same molecular evolutionary model. MrBayes 3.1.2 was run for 5,000,000 generations, sampling trees every 100 generations. We discarded the lower 25% of the trees as burn-in trees in the computation of a 50% majority rule consensus tree. Support values for inferred clades were calculated from Bayesian posteriors (percent of times a clade occurred among post burn-in trees).

Body Shape Divergence Between Predation Regimes in Bahamas Blue Holes

To evaluate lateral body shape variation across predation regimes in Bahamas mosquitofish, we digitized ten landmarks on x-ray radiograph images (following Langerhans et al., 2007) and employed geometric morphometric methods and a statistical approach described by Riesch et al. (2013). Briefly, we conducted mixed-model nested multivariate analysis of covariance (MANCOVA) using geometric shape variables (relative warps) as dependent variables, and centroid size, predation regime, and population nested within predation regime (random effect) as independent variables. To evaluate the nature of morphological variation associated with predation regime, we performed canonical analysis of the predation regime term in the model to derive a morphological vector of divergence (**d**, following Langerhans, 2009). This vector describes the linear combination of dependent variables exhibiting the greatest differences between predation regimes, controlling for other factors in the model, in Euclidean space. We visualized shape variation along this axis by regressing landmark coordinates (superimposed using Generalized Procrustes Analysis) onto **d** using tpsRegr (Rohlf, 2016). 199 of 272 specimens examined here were previously examined using the same landmarking method in Langerhans et al. (2007), but this new analysis includes new individuals collected during the same time period from six additional populations and performs a more appropriate statistical procedure developed after the original publication. Here, we found that body shape differences between predation regimes were strongly evident ($F_{15,1563} = 15.27$, $P < 0.0001$), with Bahamas mosquitofish inhabiting blue holes with the piscivorous bigmouth sleeper exhibiting a larger mid-body / caudal region and smaller head (Fig. S2). These patterns mirror those previously documented in this system, indicating that the shape divergence between predation regimes is robust across numerous populations, and consistent among multiple statistical approaches.

Results of Common-garden Experiment

We found significant effects of population, environment, and their interaction on variation in gonopodial-complex traits (Table S4). We were particularly interested in whether populations largely maintained their characteristic differences observed in the wild after rearing in a common laboratory environment (i.e. the population term), and whether the strength of these genetically-based differences was similar or greater in magnitude to environment-dependent variation among populations (i.e. the interaction term). Using Wilks's partial η^2 as an estimate of multivariate effect size (Langerhans and DeWitt, 2004), we found that the overall strength of genetically-based differences (partial $\eta^2 = 16.93\%$) exceeded that of environment-dependent variation among populations (partial $\eta^2 = 10.20\%$). By far, the strongest effect of laboratory rearing was found for the length and surface area of the gonopodium, while laboratory rearing had no influence on the expression of gonopodial anterior transposition. Most traits showed population-dependent environmental effects (Population × Environment term). The strongest population-dependent environmental effects were observed for gonopodium size and length of the 16th hemal spine, where these effects were 63-86% as strong as the main effect of population (using η^2 as an estimate of effect size). Meanwhile, some traits showed moderate but significant population-dependent environmental effects (number of hemal spines, angle of the 16th hemal spine), and other traits showed highly significant population-dependent environmental effects that were relatively small in magnitude compared to the main effect of population differences (length of 14th hemal spine, length of the 15th hemal spine, and length of the uncinate process of the 15th hemal spine).

Relative Testes Size and Gonopodial Anterior Transposition

An alternative explanation for diversity in gonopodial anterior transposition is that it is correlated with testes size, with reduced transposition accommodating larger testes. This could arise from indirect selection or architectonic associations, resulting in within-population and among-population associations between the two traits. For Bahamas mosquitofish inhabiting blue holes, prior work can help us address this notion. Prevoius research has demonstrated that fish in high-predation blue holes exhibit relatively larger testes than those in low-predation blue holes (Riesch et al., 2013; Langerhans, 2018). Thus, even though high-predation populations exhibit greater gonopodial anterior transposition (shown in this study), they do not consequentially have smaller testes—they actually show the oppostite pattern. Moreover, Riesch et al. (2020) specifically examined the relationship between lateral body shape and testes size, and found no association between the two traits even though lean weight and fat content did show significant relationships with general body form. Using pevious data, we can further provide new tests that directly investigate the relationship between gonopodial anterior transposition and relative testes size (GSI: gonadosomatic index). Using population mean values for male GSI from these prior studies, we can examine among-population associations across 17 of the 18 populations studied here, testing whether populations with larger testes show reduced gonopodial anterior transposition. We found no such association (linear regression, one-tailed $P = 0.73$). Moreover, we can calculate gonopodial anterior transposition (relative distance of anterior interior insertion of gonopodium [anal fin ray 1] to the center of the eye) for 138 individuals using these prior data on body shape (landmarks previously digitized, but this metric not calculated), and test for the predicted association with relative testes size at the inter-individual level (individuals from 14 populations). We again found no such association (one-tailed $P = 0.29$; general linear model with relative gonopodial anterior transposition as dependent variable, $\log_{10}$ SL as covariate, arcsin square-root transformed GSI as independent variable, Population as random effect). Thus, it does not appear that testes size is involved in patterns of diversification in gonopodial anterior transposition.

SUPPLEMENTARY TABLES

Table S1 | Information for specimens used in phylogenetic analyses (LLSTC = Langerhans Laboratory Specimen and Tissue Collection, housed at North Carolina State University; CPUM = Colección de Peces de la Universidad Michoacana de San Nicolás de Hidalgo).

		GenBank accession number			
Species	Collection locality	Cyt *b*	ND2	S7	Voucher
Belonesox belizanus	Amalgres, México	HM443900	HM443919	HM443938	LLSTC 04587
Heterophallus rachovii	Amalgres, México	HM443901	HM443920	HM443939	LLSTC 04584
Gambusia affinis	Mainero, México	HM443902	HM443921	HM443940	CPUM 2715
Gambusia affinis	Brazos County, Texas	HM443906	HM443923	HM443941	LLSTC 04578
Gambusia affinis	Cleveland County, Oklahoma	HM443905	HM443925	JN128635	LLSTC 04579
Gambusia affinis	Shannon County, Missouri	HM443903	HM443926	HM443942	LLSTC 04580
Gambusia aurata	Ciudad Mante, Tamaulipas, México	JX275481	JX275467	JX275474	CPUM 2312
Gambusia aurata	El Limón, Tamaulipas, México	JF437627	JF437630	JF437633	LLSTC 11425
Gambusia aurata	Forlon, Tamaulipas, México	JX275482	JX275468	JX275475	CPUM 4409
Gambusia clarkhubbsi	Val Verde County, Texas	JX275483	JX275469	JX275476	LLSTC 01787
Gambusia gaigei	Brewster County, Texas	JX275484	JX275470	JX275479	LLSTC 13468
Gambusia geiseri	Hays County, Texas	GGU18207	JX275471	JX275478	LLSTC 13467
Gambusia heterochir	Menard County, Texas	GHU18208	JX275472	JX275477	LLSTC 01442
Gambusia holbrooki	Miami-Dade County, Florida	HM443916	HM443935	HM443948	LLSTC 04582
Gambusia holbrooki	Manatee County, Florida	HM443917	HM443936	HM443947	LLSTC 04583
Gambusia holbrooki	Richland/Lexington Counties, South Carolina	HM443918	HM443937	JN128636	LLSTC 04586
Gambusia hurtadoi	Nuevo Zaragoza, Chihuahua, México	JX275485	JX275473	JX275480	CPUM 2125
Gambusia quadruncus	Ciudad Mante, Tamaulipas, México	HM443911	HM443928	HM443944	LLSTC 04572
Gambusia quadruncus	El Limón, Tamaulipas, México	HM443909	HM443930	HM443945	LLSTC 04573
Gambusia quadruncus	Llera, Tamaulipas, México	HM443912	HM443932	HM443946	LLSTC 04574
Gambusia quadruncus	Ciudad Victoria, Tamaulipas, México	HM443908	HM443927	HM443943	LLSTC 04571
Gambusia speciosa	Val Verde County, Texas	JF437628	JF437631	JF637634	LLSTC 11426

Table S2 | Standardized directional, quadratic, and correlational selection gradients on relative gonopodium length and gonopodial anterior transposition based on three separate estimates of fitness (mating success). Note that directional selection gradients were calculated and tested for significance with only linear terms in the model, while other gradients employed models with all terms included (Lande and Arnold, 1983). Quadratic terms were doubled to accurately estimate these selection coefficients (Stinchcombe et al., 2008).

	Genital Contact Success			Number of Genital Contacts			Genital Contact Efficiency		
Trait	β / γ	Std. Err	*P*	β / γ	Std. Err	*P*	β / γ	Std. Err	*P*
Relative Gonopodium Length (GL)	0.17	0.13	0.1682	0.14	0.26	0.2685	-0.03	0.15	0.8757
Gonopodial Anterior Transposition (GAT)	-0.05	0.13	0.6636	-0.29	0.26	0.1002	-0.01	0.15	0.9319
GL^2	0.17	0.22	0.2615	-0.49	0.47	0.1547	-0.01	0.27	0.9141
GAT^2	0.04	0.21	0.5355	-0.35	0.44	0.1088	0.20	0.25	0.4137
GL x GAT	**0.30**	**0.16**	**0.0293**	0.00	0.33	0.7118	**0.40**	**0.19**	**0.0406**

Table S3 | Canonical loadings for the six hemal-spine traits examined for association with gonopodial anterior transposition, describing the relationship between greater modification and elaboration of hemal spines and a more anteriorly position gonopodium (all traits $P < 0.001$).

Hemal-spine trait	Canonical Loading
Number of modified hemal spines	0.85
Length of 14th hemal spine	0.79
Length of 15th hemal spine	0.86
Length of uncinate process on 15th hemal spine	0.90
Length of 16th hemal spine	0.90
Angle of 16th hemal spine	-0.93

Table S4 | Statistical results examining the genetic basis of variation in gonopodial-complex traits in Bahamas mosquitofish.

	Population		Environment		Population × Environ.		$\log_{10}$ standard length	
dependent variable	test statistic	*P*	test statistic	*P*	test statistic	*P*	test statistic	*P*
All traits (MANCOVA)	$F_{63,1414.1} = 5.82$	<0.0001	$F_{9,250} = 54.92$	<0.0001	$F_{63,1414.1} = 3.21$	<0.0001	$F_{9,250} = 461.82$	<0.0001
Number of modified hemal spines	$\chi^2_7 = 52.58$	<0.0001	$\chi^2_1 = 38.42$	<0.0001	$\chi^2_7 = 32.64$	<0.0001	$\chi^2_1 = 0.38$	0.5371
Length of 14th hemal spine	$F_{7,275} = 10.62$	<0.0001	$F_{1,275} = 8.18$	0.0046	$F_{7,275} = 4.50$	<0.0001	$F_{1,275} = 1913.44$	<0.0001
Length of 15th hemal spine	$F_{7,275} = 8.76$	<0.0001	$F_{1,275} = 0.20$	0.6523	$F_{7,275} = 4.48$	<0.0001	$F_{1,275} = 1970.01$	<0.0001
Length of unc. process on 15th hemal spine	$F_{7,270} = 14.44$	<0.0001	$F_{1,270} = 0.02$	0.8908	$F_{7,270} = 6.09$	<0.0001	$F_{1,270} = 280.58$	<0.0001
Length of 16th hemal spine	$F_{7,275} = 11.00$	<0.0001	$F_{1,275} = 3.89$	0.0495	$F_{7,275} = 6.69$	<0.0001	$F_{1,275} = 375.84$	<0.0001
Angle of 16^{th} hemal spine	$F_{7,275} = 6.44$	<0.0001	$F_{1,275} = 5.71$	0.0175	$F_{7,275} = 3.85$	0.0005	$F_{1,275} = 0.01$	0.9385
Distance of 2^{nd} pterygiophore to eye	$F_{7,275} = 2.74$	0.0090	$F_{1,275} = 0.29$	0.5895	$F_{7,275} = 1.91$	0.0679	$F_{1,275} = 6.10$	0.0141
Gonopodium lateral surface area	$F_{4,263} = 9.64$	<0.0001	$F_{1,263} = 384.44$	<0.0001	$F_{4,263} = 6.07$	<0.0001	$F_{1,263} = 1178.55$	<0.0001
Gonopodium length	$F_{4,274} = 5.95$	<0.0001	$F_{1,274} = 206.08$	<0.0001	$F_{4,274} = 5.11$	<0.0001	$F_{1,274} = 1741.94$	<0.0001

SUPPLEMENTARY FIGURES

Figure S1 | Illustration of sexual dimorphism in poeciliid live-bearing fishes: **(A)** male, **(B)** female (*Gambusia affinis* depicted). Note the highly modified anal fin in males (gonopodium), which is positioned more anteriorly than the anal fin in females. While females have retained a relatively little-modified ancestral two-part body plan, male poeciliids have evolved a three-part body plan with the evolution of the novel ano-urogenital vertebral region.

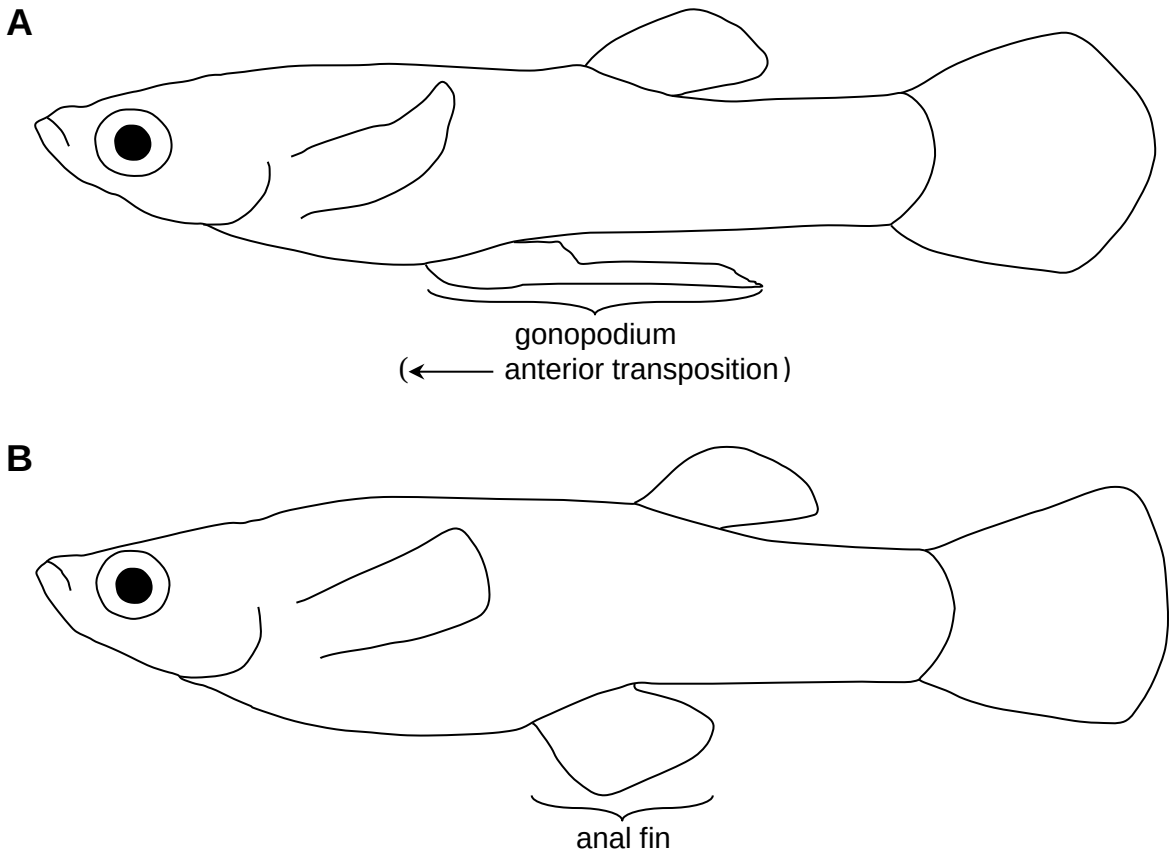

Figure S2 | Morphological divergence in male Bahamas mosquitofish between low-predation (open symbols) and high-predation (filled symbols) blue-hole populations. Body shape variation described by the divergence vector derived from the predation regime term of the MANCOVA, illustrated using thin-plate spline transformation grids relative to mean landmark positions (observed range of variation depicted; i.e., no magnification). Solid lines connecting outer landmarks are drawn to aid interpretation. Circles along the divergence vector represent population means. Representative radiographs of individuals from low-predation and high-predation populations are provided below the axis (individuals selected from two blue holes separated by only 0.3 km of terrestrial habitat). Note the larger mid-body / caudal region, smaller head, more anteriorly positioned gonopodium, and longer and more numerous modified haemal spines in high-predation populations.

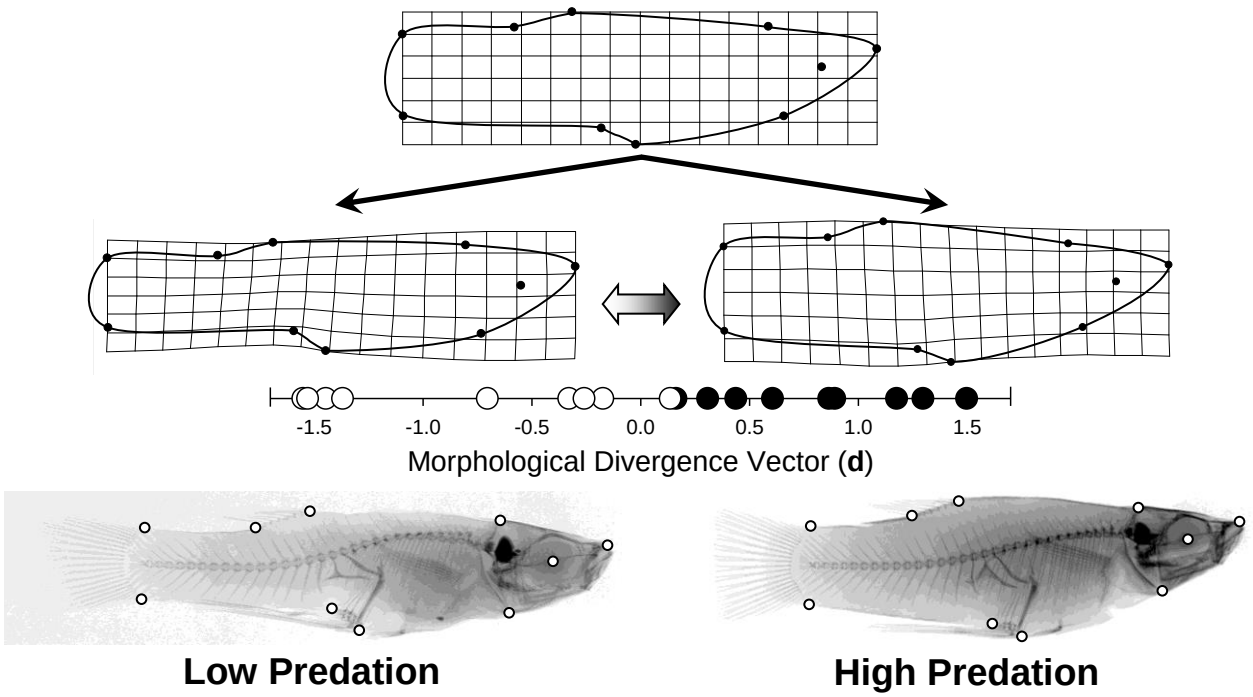

Figure S3 | Map of 18 blue holes where Bahamas mosquitofish were collected (blue holes without piscivorous fish: blue circles, labels beginning with "L"; blue holes with piscivorous fish: red circles, labels beginning with "H").

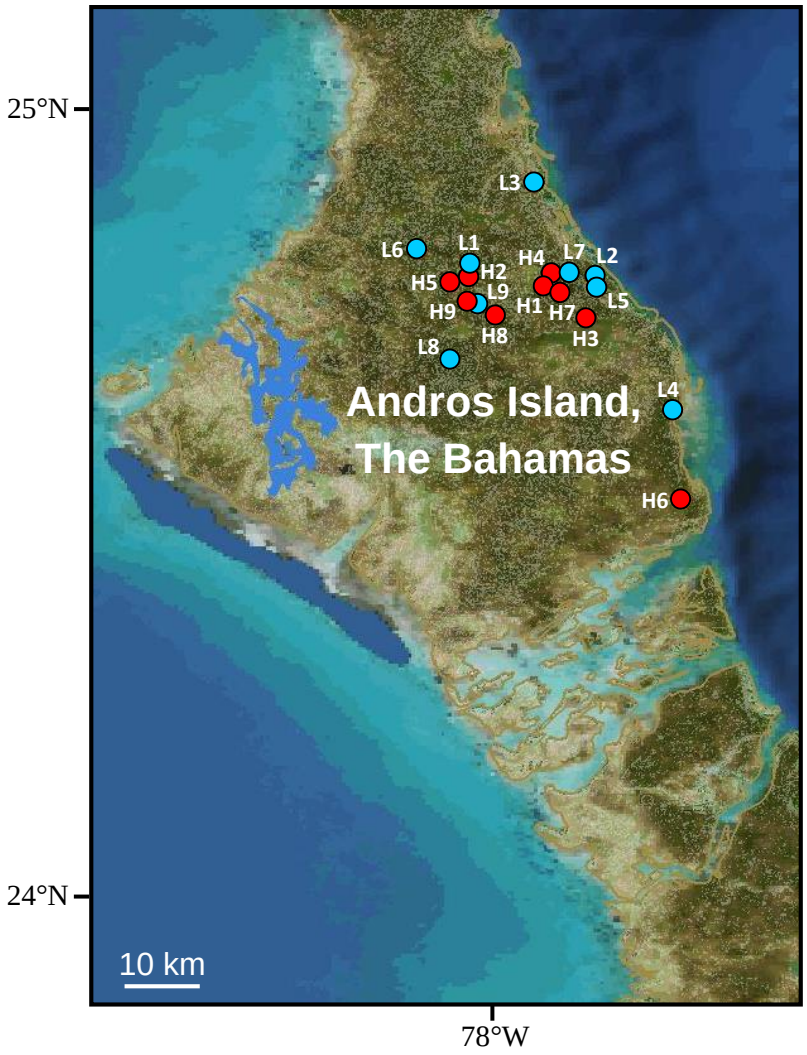

Figure S4 | Differences between low-predation (open bars) and high-predation (filled bars) populations of Bahamas mosquitofish in **(A)** length of the 14th hemal spine (one-tailed P = 0.0179), **(B)** length of the 15th hemal spine (one-tailed P = 0.0016), **(C)** length of the 16th hemal spine (one-tailed P = 0.0002), **(D)** length of the uncinate process on the 15th hemal spine (one-tailed P = 0.0009), **(E)** angle of the 16th hemal spine (one-tailed P = 0.0002), and **(F)** gonopodium length (one-tailed P = 0.9308). Least-squares means ± one standard error depicted (for length variables, mm units back-transformed from $\log_{10}$-transformed data used in analyses).

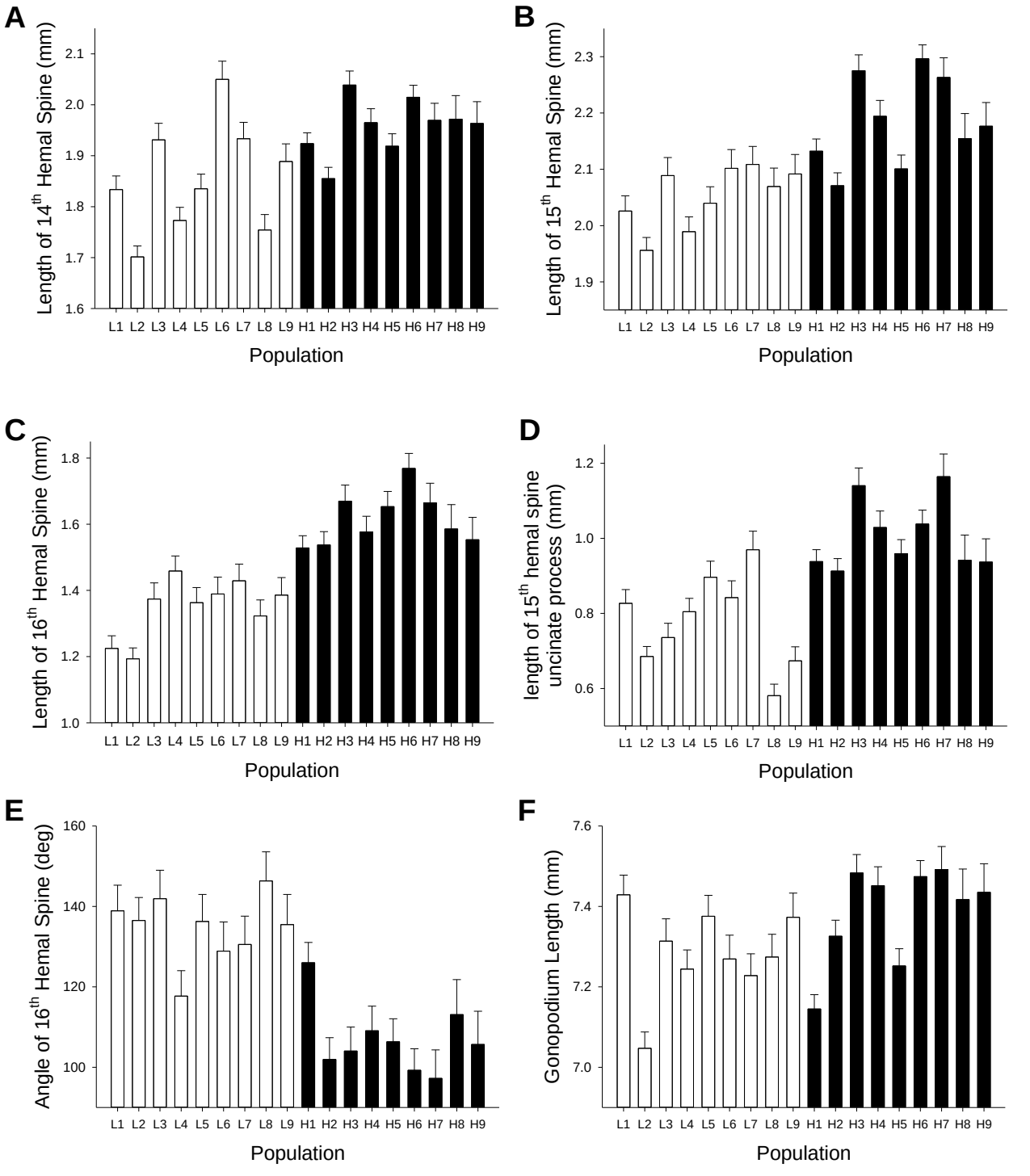

SUPPLEMENTARY REFERENCES

Evans, J. P., Pilastro, A. and Ramnarine, I. W. (2003). Sperm transfer through forced matings and its evolutionary implications in natural guppy (*Poecilia reticulata*) populations. *Biol. J. Linnean Soc.* 78, 605-612.

Lande, R. and Arnold, S. J. (1983). The measurement of selection on correlated characters. *Evolution* 37, 1210-1226.

Langerhans, R. B. (2009). Trade-off between steady and unsteady swimming underlies predator-driven divergence in *Gambusia affinis*. *J. Evol. Biol.* 22, 1057-1075. 10.1111/j.1420-9101.2009.01716.x

Langerhans, R. B. (2018). Predictability and parallelism of multitrait adaptation. *J. Hered.* 109, 59-70. 10.1093/jhered/esx043

Langerhans, R. B. and DeWitt, T. J. (2004). Shared and unique features of evolutionary diversification. *Am. Nat.* 164, 335-349. 10.1086/422857

Langerhans, R. B., Gifford, M. E. and Joseph, E. O. (2007). Ecological speciation in *Gambusia* fishes. *Evolution* 61, 2056-2074. 10.1111/j.1558-5646.2007.00171.x

Posada, D. (2008). jModelTest: phylogenetic model averaging. 25, 1253-1256. 10.1093/molbev/msn083

Riesch, R., Martin, R. A. and Langerhans, R. B. (2013). Predation's role in life-history evolution of a livebearing fish and a test of the Trexler-DeAngelis model of maternal provisioning. *Am. Nat.* 181, 78-93. 10.1086/668597

Riesch, R., Martin, R. A. and Langerhans, R. B. (2020). Multiple traits and multifarious environments: integrated divergence of morphology and life history. *Oikos* 129, 480-492. 10.1111/oik.06344

Rohlf, F. J. 2016. TpsRegr. Stony Brook: Department of Ecology and Evolution, State Univ. New York.

Ronquist, F. and Huelsenbeck, J. P. (2003). MrBayes 3: Bayesian phylogenetic inference under mixed models. *Bioinformatics* 19, 1572–1574. 10.1093/bioinformatics/btg180

Schupp, I. and Plath, M. (2005). Male mate choice and sperm allocation in a sexual/asexual mating complex of *Poecilia* (Poeciliidae, Teleostei). *Biol. Lett.* 1, 169-171. 10.1098/rsbl.2005.0306

Stinchcombe, J. R., Agrawal, A. F., Hohenlohe, P. A., Arnold, S. J. and Blows, M. W. (2008). Estimating nonlinear selection gradients using quadratic regression coefficients: double or nothing? *Evolution* 62, 2435-2440. 10.1111/j.1558-5646.2008.00449.x